Propulsion mechanisms of catalytic nanomotors

Author: Eric Babià Soler
Advisor: David Reguera Lopez
Facultat de Física, Universitat de Barcelona, Diagonal 645, 08028 Barcelona.*

Abstract: This project aims to study a bimetallic rod-shaped nanomotor self-propeled in hydrogen peroxide solutions. Here we present governing equations and numerical simulations using COMSOL Multiphysics®, which shows that bimetallic rod is driven by electrical body forces which are generated from an asymmetric ion flux mechanisms. It is believed that this type of locomotion is commonly used by microorganisms, and in the near future these artificial nanomotors can have several applications, from environmental remediation to drug delivery.

I. INTRODUCTION

Increasingly technology tends to reduce the size of the objects that we create: microelectronic, micro sensors… Nowadays the next step leads to nanometric scales. In the future, robots will reach this nanometric size, and they will need motors in order to move around. For this reason, inspired by nature, there is a growing interest in engineering artificial machines which can swim autonomously, imitating molecular motors in living organisms. In nature we can find different examples of efficient biological motors that can do complex tasks autonomously converting chemical reactions into movement. Some examples of these processes are cell division, DNA transcription, protein synthesis, and cell migration[6]. The locomotion of microorganisms is commonly attributed to mechanical deformation of appendages, like flagella, although Mitchell[7] proposed that an asymmetric ion flux on a bacterium's surface could generate electric fields that drive locomotion via self-electrophoresis. For instance, cyanobacteria are able to swim at speeds near 25μm/s without flagella[4].

Recent advances in nanofabrication have enabled to engineer synthetic microorganisms like the proposed by Mitchell that can swim due to asymmetric ion flux mechanisms.

Phoretic transport is the movement of colloidal particles by a gradient that interacts with the surface of the particle, therefore we can distinguish by the applied field, usually electrical potential (electrophoresis), concentration of molecules (diffusiophoresis), or temperature (termophoresis). In our study, we are specifically interested in locomotion of particles that move due to potential gradients (electrophoresis) and concentration generated by reactions on the particle surface. The forces caused by diffuphoresis of the concentrations studied are several orders of magnitude smaller than electrophoresis[4]. We fixed the temperature of the fluid thus there is no contribution from thermophoresis.

The aim of this project is to analyse this type of nanomotor, which can be either linear or rotatory motors. In this case, our study is focused on the study of the first ones: linear biomotors. In this work we analysed bimetallic rod-shaped nanomotors changing their geometry and the materials proportion in order to have the optimum configuration.

Here we present governing equations and numerical simulations that describe the motion of a half of gold (Au) and half of platinum (Pt) motor in hydrogen peroxide (H_2O_2), where peroxide is the fuel in this type of motors. We do not give a full explanation of the model, we rather show a generic description allowing to extract the main features of the physics involved. To solve the equation based on Poisson-Nerst-Planck-Stokes by numerical simulations we used COMSOL Multiphysics®.

II. METHODS

Below are shown the equations that are involved in the simulation. As we can see in Figure 1, the H_2O_2 is oxidised at the bottom of the anode (Pt) and generates protons (H^+), electrons and diatomic oxygen (O_2). These electrons move through the rod to the cathode (Au), and by a reduction reaction, combine protons, oxygen and peroxide. This specific geometry and the chemical reactions involved generate a dielectric dipole and an electric field pointing from the anode to the cathode. The electric forces drive the surrounding fluid and give motion to the nanorod.

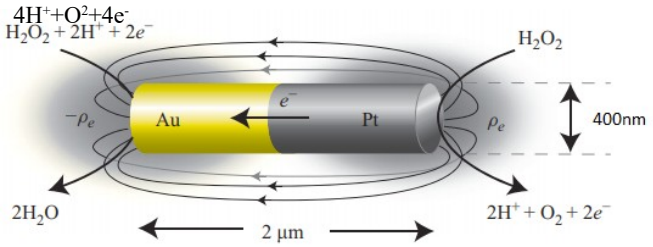

FIG. 1: Picture readapted form [4] of the rod-shaped nanomotor made with Au and Pt in a solution of H_2O_2, with the dimensions that we used. It also shows the chemical reactions, an intuitive cloud of a charge distribution, the transport of electrons, and the approximate electric field lines. These conditions will drive the nanomotor to the right.

A. Governing equations

The physics involved in this study include chemical reactions, electrostatic, transport of charged species, and fluid dynamics, all together. For this reason, the resolution of this set of equations can not be done analytically and we had to use the simulations.

First of all, we have to solve the advection, the diffusion and electromigration of the species involved when we are working with charged solution surrounding the nano-rod. Here is the equation required:

$$u\cdot\nabla c_i=\nabla\cdot\left(D_i\nabla c_i+z_i F v_i c_i\nabla\Phi\right), \qquad (1)$$

Where c is the concentration of charged species, u is the velocity, Φ is the electrostatic potential, F is the Faraday constant and the subscript i refers to the species. In this case, these species are protons and hydroxide ions due to the fact that peroxide and oxygen are electrically neutral so they do

* Electronic address: ebabiaso7@alumnes.ub.edu

not have any influence. For this reason, we do not consider them in the previous equation. Further more z_+ equals 1 for the protons and z_- is -1 for the hydroxide ions. Diffusivity (D_i) and mobility (ν_i) are connected by the Einstein-Smoluchowski relation, $D_i=\nu_i RT$, where R is the ideal gas constant and the temperature (T) is 293.14K throughout the domain.

The electrostatic potential depends on the local free charge density and follows the Poisson equation:

$$-\varepsilon \nabla^2\Phi=\rho_e=F\sum_i z_i C_i, \qquad (2)$$

Here, we define the permittivity as $\varepsilon=\varepsilon_r\varepsilon_0$ and we use the dielectric value of water (ε_r).

The dynamics of the fluid is described by the Navier-Stokes equation:

$$\nabla\cdot u=0$$
$$\rho(u\cdot\nabla u)=-\nabla p+\eta\nabla^2 u-\rho_e\nabla\Phi \qquad (3)$$

Where $\nabla\cdot u=0$ denotes the incompressibility of the fluid, ρ is the fluid density, p is the pressure, η is the dynamic viscosity, and the last term of the equation (3) is the electrical force.

B. Implementation COMSOL®

COMSOL Musltiphysics® is a software of analysis and resolution by finite elements of a mesh for several physical applications, especially coupled phenomena, as in this case. Its function is to discretize equations and to solve them by using specific algorithms.

As mentioned before, to solve the equations system (1)-(3) numerically using COMSOL®, the reactions have to be represented by boundary conditions.

On the anode and cathode the flux of the normal vector is pointing outward from the surface of the rod, and after few approximations[3,4] the electrochemical currents become:

$$j_{anode}=k_{anode}c_{H_2O_2},$$
$$j_{cathode}=k_{cathode}c_{H_2O_2}c_+^{\,2}, \qquad (4)$$

Where, k_{anode} and $k_{cathode}$ are the effective rate constants. To avoid charge accumulation, and to maintain the number per unit time of protons released in the solution equal to the number per unit time of protons consumed, we impose:

$$J_{total}=\int_{anode} j_{anode}\,dA+\int_{cathode} j_{cathode}\,dA=0, \qquad (5)$$

In order to verify our simulation comparing with previous study, we used the following simplification:

$$j_0=j_{anode}=-j_{cathode} \qquad (6)$$

At the motor surface we apply a non-slip condition $u=0$, and the surface potential at low salt concentrations is $\Phi=\zeta$. Moreover, far from the rod this potential prevails zero and the concentration reaches the bulk value.

Considering the hydroxide ions flux over the outward of the motor, the contribution of diffusion, electromigration and convection is zero:

$$-D_-\nabla c_- - z_- F\nu_- c_-\nabla\Phi+c_- u=0, \qquad (7)$$

On the other hand, the flux of protons at the anode and at the cathode corresponds to:

$$-D_+\nabla c_+ - z_+ F\nu_+ c_+\nabla\Phi+c_+ u=\begin{cases} j_{anode} \\ j_{cathode}\end{cases}, \qquad (8)$$

Assuming that the flow is axisymmetric and to make the work easier with the geometry of the nanomotor we solved the system over 2-Dimensions instead of the 3-Dimensions. The domain through all the simulation is 6x14 μm^2 and is discretized in a triangular mesh, with more resolution near the rod than in the farthest solution, were there are negligible gradients, hence we save time in computation. The nano-rod simulated has a radius (r) of 200 nm and a length (l) of 2 μm.

Working with nano-size means a low Reynolds number, eq. (8), then inertia can no longer sustain motion, and any external force is counterbalanced by the viscous force. The system reaches its terminal velocity quickly, that is the reason why we work with steady solutions.

$$Re=\frac{\rho\cdot u\cdot l}{\eta}=\frac{Inertial\ forces}{Viscous\ forces}\lesssim 1, \qquad (9)$$

Where, l denotes the dimensions of the rod.

The main constants used in the simulation are shown in the table 1, the other parameters that do not appear in the table as the concentration of peroxide(c_{H2O2}), the zeta potential(ζ), or the concentration of protons and ions (c_+, c_-) are changed during the whole study.

Parameter	Value
Solution dielectric constant	$\varepsilon_r=78.4$
Rate constant of the anode	$k_{anode}=5.5\cdot10^{-9}$ m/s
Rate constant of the cathode	$k_{cathode}=1$ m^7/s·mol^2
Protons diffusivity	$D_+=9.311\cdot10^{-9}$ m^2/s
Hydroxide ions diffusivity	$D_-=5.273\cdot10^{-9}$ m^2/s
Peroxide diffusivity	$D_{H2O2}=6.6\cdot10^{-10}$ m^2/s
Solution viscosity	$\eta=8.9\cdot10^{-4}$ Pa·s
Solution density	$\rho=998$ kg/m^3
Faraday constant	$F=69485$ s·A/mol

TABLE I: Values of the main parameters for the simulation of the nanomotor taken from the reference[4]. The value of the parameters that are not included were modified during the study.

III. RESULTS

Below are shown the results of the simulations for three different studies. In the first one, we present the results of a charged rod modifying the concentration, surface potential and concentration of ions. After that, we varied the geometry of the motor. Finally, in the last study, the Au/Pt proportion was changed.

Figure 2.a shows the simulated concentration of protons, where the arrows indicate the direction of the fluid that flows from the anode (grey) to the cathode (gold colour). The Figure 2.b, illustrates the simulated spatial variation of the potential, where the arrows indicate the direction of the electric field. Finally, the Figure 2.c shows the resulting velocity field, where the fluid velocity is zero at the nano-rod surface (blue colour), as required by the no-slip condition, and the maximum value is at the bulk solution (red colour)

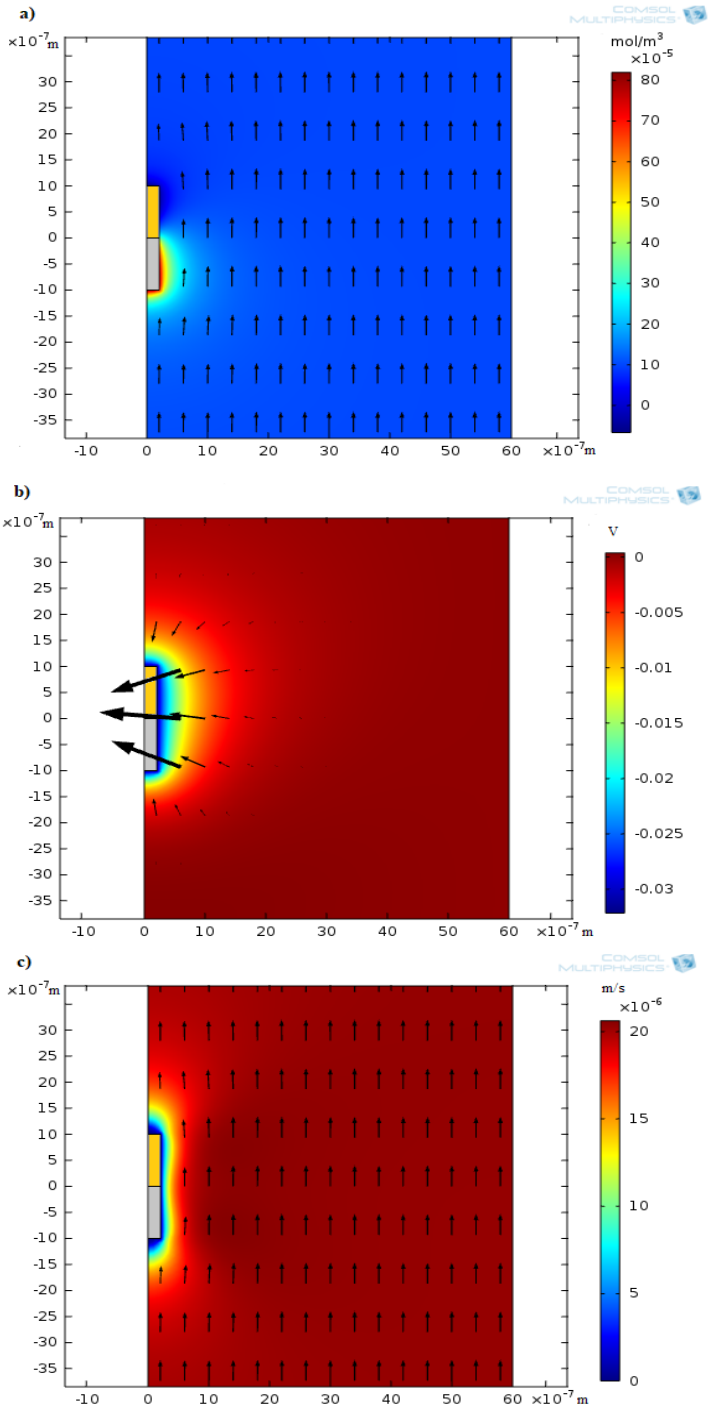

FIG. 2: Simulation results obtained using COMSOL® with the values in Table 1, and the simplification (6). Here, the surface potential (ζ=-32.15 mV), the bulk concentration of hydrogen peroxide (c_{H2O2}=1500 mol/m^3) and the bulk concentration of protons and the hydroxide ions (c=10^{-4} mol/m^3) are fixed. (a) The concentration of protons, where the arrows indicate the direction of the flow, (b) The surface potential (ζ), and the electric field (arrows), (c) The velocity field where the maximum value is 20.5 μm/s, and the minimum, obeying the no-slip condition at the nanomotor surface, is zero.

Looking at the charge distribution, there is more positive charge accumulation on the anode, where the protons are being generated, and depleted at the cathode, where they are being consumed. The electric potential is not completely symmetric due to this excess of charge accumulation on the anode. The electric field is particularly intense near the rod, where the potential gradient is more pronounced. In absence of reactions (without peroxide) both proton concentration and electrical potential are axisymmetric.

These simulations show which is the mechanism that enables it to move. The chemical reactions on the anode and the cathode, as we said, build up a gradient of protons, Figure 2.a, allowing the appearance of a diffusion current that generates an electric field, equation (1), which drives the fluid motion. By Galilean invariance, this is the same as the nano-rod moving with the platinum forward.

We used the fluid velocity far from the rod, as a measure of the motor speed, where the fluid velocity reach a maximum value of 20.5 μm/s which corresponds to 10 body lengths per second.

The velocity profile has a strong symmetry because of the low Reynols number, eq (9), and the appearance does not change for other values of hydrogen peroxide concentration.

A. Simulation validity

In order to verify the validity of our simulation we introduced the same values of the concentration of hydrogen peroxide and the zeta potential as the reference [1], and we plotted it in Figure 3. We also examined that, indeed, the velocity decreases linearly to zero for different surface potentials, following the scaling analysis proposed by Moran[1,4]:

$$v \propto \frac{\zeta F l \lambda_D}{\eta D_+} j, \qquad (10)$$

Where l is again the dimension of the nanomotor, and the Deby thickness (λ_D) in our simulation is around 1μm. Whereas all the parameters are constants, the velocity (v) goes directly proportional to the zeta potential (ζ). This expression predicts that the velocity should increase linearly with the surface potential and the reaction flux. At the same time the reaction flux also goes linearly with the peroxide concentration, equation (4). Plotting the linear regression shows in effect that all y-intercept intersect the zero velocity, but with different slop.

Further we changed to positive the surface potential and the results were similar to the ones that appear in Figure 3 but in the opposite side of the graphic, where the nano-rod inverts its direction (in agreement with the predictions of Moran, Wheat and Posner [1]).

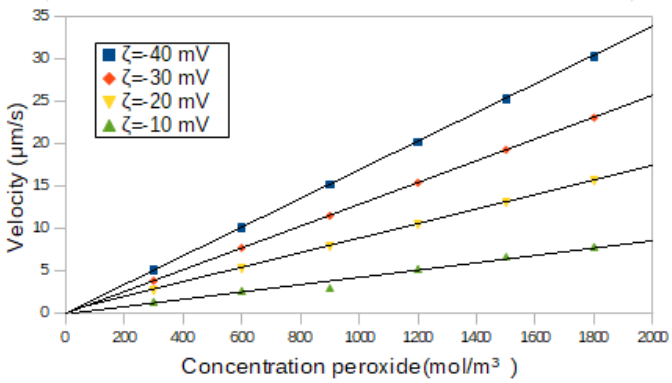

FIG. 3: Results of the nano-rod velocity according to the concentration of hydrogen peroxide simulated with different surface potentials (ζ) and the respective linear regression.

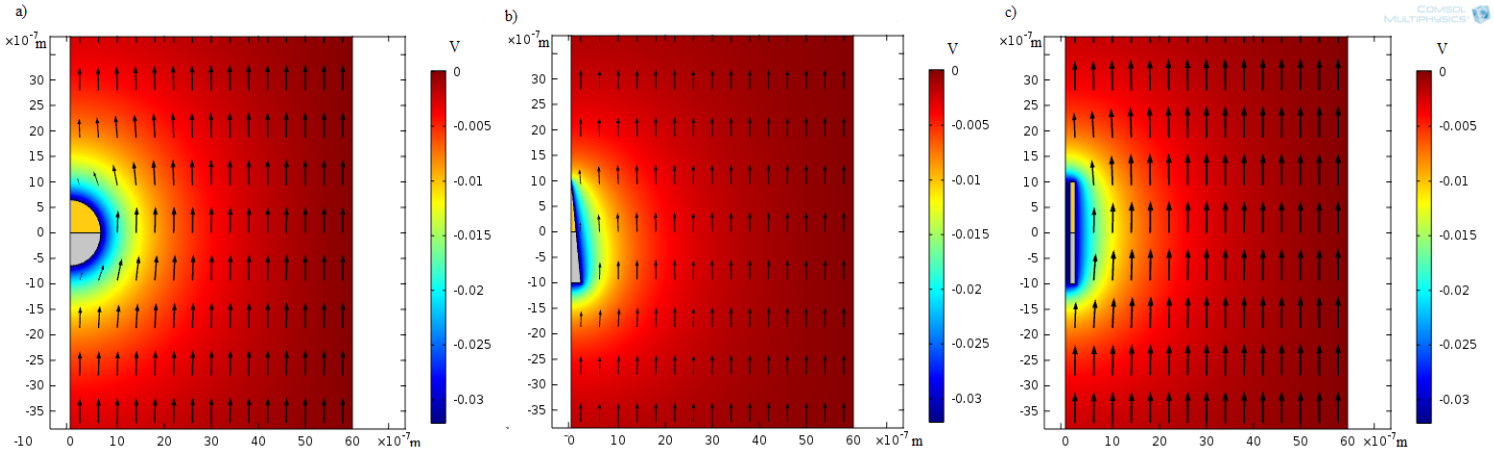

FIG. 4: Simulation results obtained using COMSOL® with the values in Table 1, and the equation (4) for the ion flux. Here, the surface potential (ζ=-32.15 mV), the bulk concentration of hydrogen peroxide (c_{H2O2}=1500 mol/m³) and the bulk concentration of protons and the hydroxide ions (c=10^{-4} mol/m³) are fixed. (a) The surface potential (ζ) for a sphere instead of a rod, (b) The surface potential (ζ) for a cone shape instead of a rod, (c) The surface potential (ζ) for a hollow cylinder instead of a rod. Here, the arrows indicate the direction of the flow, with the same scale factor for the three representations.

Figure 3 proves, as it would be expected, that hydrogen peroxide is the fuel that drives this motor, its concentration controls the rate of the reactions at the anode and cathode. We assume that the oxygen generated by reactions in this range of peroxide concentration does not reach the saturation limit, so bubbles do not appear[4]. However the increase of this fuel concentration is not linear in the whole range, this means that at high peroxide concentrations the velocity reaches a saturation[4].

We did not show the plot changing the bulk concentration ions because, as it was expected, it follows the same behaviour as figure 3, and the velocity increases in direct relation to the concentrations of ions on the solution.

Thus, we can see that our results of velocity, concentration, and surface potential compared with other studies and experiments[1,4] have a strong agreement. In other words, our simulation is valid.

B. Geometry

Since the main objective of this study is to know which factors optimise the velocity of the motor, we analysed the geometry and the proportion of Au and Pt.

Knowing that our simulation results show a good agreement with scaling analyses and experiments measurements[4], we can change the geometry in order to know which goes faster. In Figure 4 we represented the most representative plots of these different motors.

We realised that the faster motor was the hollow cylinder (Figure 4.c) with a velocity of 31.7 μm/s (15 body lengths per second) while the whole cylinder, with the same radius and the same length, moves with a velocity of 25.8 μm/s. The hollow cylinder is faster due to the fact that the its structure doubles the whole rod surface, the outer and the inner ones, but it is not two times faster. As we have seen, this type of motors propelled by electrophoresis need the chemical reactions on the anode and the cathode to build up a gradient of protons and an electric field.

To proof this hypothesis we simulated a sphere with the same area as the whole cylinder. The speed of these two configurations results to be similar, 26.1μm/s for the sphere and 25.8 μm/s for the whole cylinder, even though the drag coefficient of both configurations is different. The drag coefficient for the sphere is around 0.47, and for the whole cylinder is near 0.82. Working at low Reynolds number the geometry of the motor has no big contributions. The evidence is that the velocity of this sphere (26.1 μm/s) has no meaningful difference related to the velocity of the rod (25.8 μm/s).

On the other hand, we plotted a cone (Figure 4b) with the same length and base radius as the original rod. Now the velocity decreased to 19.6 μm/s. Surprisingly, although we said that the shape geometry no cause appreciable changes on the velocity of the motor, if we reverse the cone, the velocity decreases to 10.2 μm/s.

C. Au-Pt proportion

Interestingly, trying to understand the gap of velocities between the cone and the inverted cone, we realised that the proportion of gold and platinum influences the velocity.

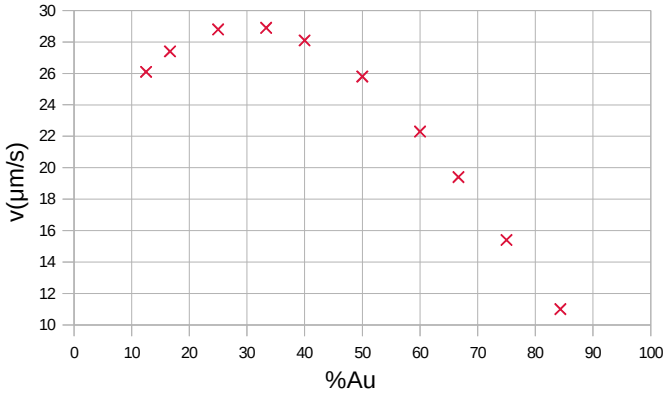

FIG. 5: Nano-rod velocity as a function of the rate of gold-platinum, with the same values used in Figure 4.

Figure 5 shows the velocity of the fluid with different proportions of Au-Pt. We believed that the optimum proportion could be fifty-fifty. Nevertheless, we found that the fastest proportion is close to the 30% Gold and 70% platinum. This could be due to difference of the ion flux, equation (4), where the consumption and the generation of protons are asymmetric. In consequence, back to the study of

geometry, the normal cone has less gold than the inverted one. Following this argue, this could be possible.

IV. CONCLUSIONS

- We have shown that the electric field that drives the nanomotor exist due to the diffusive proton flux between the anode and cathode. In addition, we have seen that the proportion of gold and platinum has an influence on the electric field and hence on the motor velocity. Other parameters have a more obvious influence, like the bulk concentration of ions, and the concentration of peroxide.
- In order to control the direction motion of these nanomotors, a ferromagnetic component could be introduced between platinum and gold. Thus, we can orient the engine to a specific target by using an external magnetic field.
- The application of these nanomotors could be very broad. For instance, it could have a biomedical function as a drug delivery in a human body. However, the use of H_2O_2 as a fuel of these nanomotors is not biocompatible. In the future, the research of novel fuel that reacts with the bimetalic motor can contribute in the treatement of a lot of diseases.
- In the future, it would be interesting to change metals found in the motor in order to study the rate constant behaviour.
- Despite the big progresses in nanotechnology, the production methods on this scale still being quite slow and expensive. For this reason, this kind of simulations simplify the work and help us to understand these nanomotors allowing us to optimise their design.

Acknowledgments

I would like to thank my advisor David Reguera for his support and patience, as well as for introducing me to this amazing field and helping me to understand it. I would also like to thank my friends and relatives for always being there.

[1] J.L. Moran, P.M. Wheat, and J.D.Posner, *Locomotion of electrocatalytic nanomotors due to reaction induced chargeautoelectrophoresis*, PHYSICAL REVIEW E **81**, 065302(R), 2010

[2] A. Afshar Farniya, M.J. Esplandiu, D.Reguera, and A. Bachtold, *Imaging the Proton Concentration and Mapping the Spatial Distribution of the Electric Field of Catalytic Micropumps*, PHYSICAL REVIEW LETTERS **11**, 168301, 2013

[3] M.J. Esplandiu, A.Afshar Farniya, and D.Reguera, *Key parameters controlling the performance of catalytic motors*, The Journal of Chemical Physics **144**, 124702, 2016

[4] J.L. Moran, P.M. Wheat, and J.D.Posner, *Electrokinetic locomotion due to reaction-induced charge auto-electrophoresis*, Journal of Fluid Mechanics, 680, pp 31-66, 2011

[5] John L. Anderson, *Colloid Transport by Interfacial Forces*, 15213

[6] S. Sánchez, Ll. Soler, and J. Katuri, *Chemiclly Powered Micro-and Nanomotors*, Angewandte Chemie International Edition, **54**, 1414-1444, 2015

[7] P. Mitchell, *Self-electrophoretic locomotion in microorganisms–bacterial flagella as giant ionophores*, FEBS Lett. **28** (1), 1-4, 1972